



Puchalsky C., Megli T., Tiller M., Trask N., Wang Y., Curtis E.:  
**Modelica Applications for Camless Engine Valvetrain Development**  
2<sup>nd</sup> International Modelica Conference, Proceedings, pp. 77-86

Paper presented at the 2<sup>nd</sup> International Modelica Conference, March 18-19, 2002,  
Deutsches Zentrum für Luft- und Raumfahrt e.V. (DLR), Oberpfaffenhofen, Germany.

All papers of this workshop can be downloaded from  
<http://www.Modelica.org/Conference2002/papers.shtml>

*Program Committee:*

- Martin Otter, Deutsches Zentrum für Luft- und Raumfahrt e.V. (DLR), Institut für Robotik und Mechatronik, Oberpfaffenhofen, Germany (chairman of the program committee).
- Hilding Elmqvist, Dynasim AB, Lund, Sweden.
- Peter Fritzson, PELAB, Department of Computer and Information Science, Linköping University, Sweden.

*Local organizers:*

Martin Otter, Astrid Jaschinski, Christian Schweiger, Erika Woeller, Johann Bals,  
Deutsches Zentrum für Luft- und Raumfahrt e.V. (DLR), Institut für Robotik und  
Mechatronik, Oberpfaffenhofen, Germany

# Modelica Applications for Camless Engine Valvetrain Development

Christopher Puchalsky, Thomas Megli, Michael Tiller, Nate Trask,  
Yan Wang, Eric Curtis  
Ford Motor Company

## Abstract

Several variable valvetrain technologies are being aggressively pursued to increase vehicle fuel economy and reduce engine exhaust emission levels. Electromechanical Valve Actuation (EMVA) is a promising alternative that uses electromagnetic actuators to replace the conventional camshaft and provide fully flexible valve timing control. This "camless" valvetrain provides new opportunities and challenges for engine control optimization. In this work, we present two Modelica applications for EMVA development.

Control and prediction of the Air to Fuel (A/F) ratio in a port fuel injected spark-ignited (PFI SI) engine is an important factor for emissions, performance, and fuel economy. A Modelica model to simulate the dynamic behavior of fuel vaporization and storage inside a PFI SI engine has been developed. This "wall wetting" model was developed from an existing FORTRAN based model and employs several control volumes to represent fuel in various phases and locations in the engine. A multi-component fuel model (i.e. containing different constituents with a wide range of molecular weights) is used where the fuel component masses are the state variables and the mass flow rates are the flow variables. The fuel model can be easily re-declared so that different numbers and types of fuel components can be used to simulate the distillation characteristics of various fuels. For the control volumes that represent liquid fuel puddles, the connectors have additional information such as puddle area, puddle height, fuel component vapor pressure, puddle temperature, and puddle heat transfer. The processes of fuel injection, vaporization, liquid flow, and shattering are used to move fuel between the various control volumes. The Modelica model can be coupled by various degrees to engine simulation models. By comparison, in the original FORTRAN model, engine operating inputs to the wall wetting model were made by rough approximation with no opportunity for feedback from the wall wetting model to affect the operating conditions. In this application we fully couple the wall wetting dynamics to a single cylinder engine model. The complete model is then more generally applicable to the increased number of degrees of freedom afforded by the variable valve

timing control. The engine model incorporates a simple valve actuator model to replace the conventional camshaft motion with the flexible timing and transition characteristics of EMVA. The engine model predicts gas flows, temperatures, and pressures that were inputs to the FORTRAN wall-wetting model. The wall wetting model then determines the fuel vaporization rate, which in turn determines the A/F ratio input to the engine model. This subsequently changes the temperatures, pressures, and flows in the combustion chamber and port sub-models. Initial comparison of results to the FORTRAN model show reasonable agreement in A/F prediction but the FORTRAN version currently runs faster.

The other use of Modelica involves actuator development. Actuator design and control is a significant challenge for EMVA engines. To achieve performance, durability and fuel economy objectives, valve motion must be carefully controlled via electromagnets to achieve both fast transitions and low contact velocities. The actuator system must also be designed to minimize electrical power consumption. A detailed actuator model is developed to study valve transition characteristics. The model incorporates mass, spring, and electrical elements from the Modelica standard translation and electrical sub-libraries. A detailed sub-model of a solenoid with an "E-shaped" core has been developed to predict magnetic forces and inductive characteristics. The magnetic force is coupled to a reciprocating mass which represents the armature and valve assembly. Various actuator design modifications have been investigated. The effect of a simple voltage control scheme on valve motion is investigated here.

## Introduction

The global automotive industry is under increasing pressure from governmental, consumer, and non-governmental groups to improve the fuel economy of motor vehicles. Reasons for improvement range from concerns about global warming to the need to reduce the dependence on foreign, and often volatile, petroleum sources. Consumer demand and competitive

forces demand that improvements in fuel economy not be accompanied by decreases in other metrics of vehicle performance – safety, power, interior space, emissions, price, and NVH. It is often required that these other metrics improve along with fuel economy.

One group of technologies that holds promise for improving fuel economy while maintaining or improving most other areas of vehicle performance is variable valve timing (VVT). VVT reduces or eliminates many of the tradeoffs between low and high speed torque, fuel economy, idle quality, and emissions that are currently made with fixed valve timing. VVT includes current production technologies like variable cam timing, cam switching, and variable valve lift. All of these technologies use a cam to open and close the valves. A new VVT technology that holds promise is Electromechanical Valve Actuation (EMVA). EMVA uses electromagnets to open and close the valves. The valve timing is then independent of crankshaft position, and valve opening and closing times can be optimized to reduce throttling losses and to control residual gas fractions. Additionally, valves may be deactivated to reduce power consumption or to deactivate cylinders for improved fuel economy.

EMVA presents several engineering challenges in which modeling plays an important role. One such area is the development of strategies for transient air fuel control. We will discuss the development of the plant model to predict liquid fuel dynamics. Another engineering challenge is the development of the electromagnetic actuator. Both will be discussed and results will be presented.

## Wall Wetting Model Development

Prediction of transient fuel dynamics is difficult with conventional port fuel injected (PFI) engines running at fixed valve timing. In PFI engines, a fuel injector is placed in the intake port as close to the intake valve as packaging will allow. A schematic of the fuel injection and wall wetting process in a standard camshaft engine is shown in Figure 1. Fuel is injected towards the intake valve and port walls just before intake valve opening. Some fuel becomes entrained in the air stream, but most lands on the valve and port where it forms small "puddles". The fuel evaporates off the hot port walls (~95 C) and the hotter intake valve (~175 C). The fuel, gasoline, is composed of many different chemical species with widely different characteristics. The lighter, more volatile, components will evaporate easily while the heavier, less volatile, components will tend to evaporate slowly and stay in the puddle. The evaporation rate increases dramatically when the intake valve is open and the air speed in the port is high. The high air speed in the port also produces a forward flow phenomenon, which causes some of the liquid fuel on the port walls and the intake valve to be sucked into the

combustion chamber where it forms a puddle. Additionally, right at the moment of intake valve opening, the pressure in the intake port is much less than that in the cylinder. This produces a backflow pressure wave that splatters some of the fuel off of the valve and up into the port. In both the forward and backward flow processes some of the fuel is entrained in the air stream before it lands.

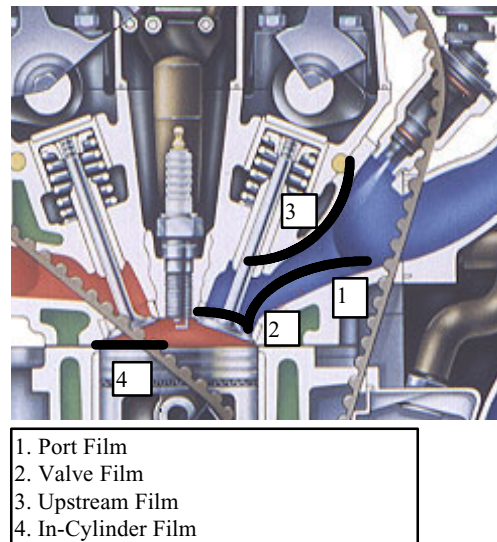


**Figure 1: Schematic of Fuel Injection.**

Prediction of transient air fuel dynamics becomes even more difficult under certain EMVA engine operating modes (e.g. late intake valve closing (IVC), alternating valve closing, and cylinder deactivation). A detailed wall wetting model to predict transient air fuel dynamics has been created in Modelica. A starting point for the Modelica model was a FORTRAN model developed by Curtis, *et. al.* [1]. The FORTRAN wall wetting model contains models of all of the processes described above, all of which have also been implemented in the Modelica version. Additionally, the Modelica version is also tied to an engine cycle simulation that provides data such as air speeds, pressures, and temperatures to the wall wetting model. The FORTRAN version used approximations for this data.

## Basic Models

In the most basic form, the wall wetting model is a collection of fuel puddles (control volumes) linked together by processes that move fuel between the various puddles. This is similar to modeling in the thermal domain where a series of thermal capacitances

exist with thermal resistances and convective elements to move the thermal energy between them.

The control volume model has the following connector instantiated as `cv` (control volume):

```
connector MassConnector
  import Modelica.SIunits;
  parameter Integer n "# of species";
  parameter String FuelNames;
  SIunits.Mass m[n];
  flow SIunits.MassFlowRate mdot[n];
end MassConnector;
```

The control volume model also contains the following equation to link the flow and across variables:

```
der(cv.m) = cv.mdot;
```

A multi-component fuel model is used. The number, type, and injected mass fraction of each component (species) is selected to match the distillation characteristics of the fuel. There are 21 chemical species from which to select. The fuel model contains both fuel composition and material property data. It has the following code:

```
model Fuel
  extends FuelIcon;
  replaceable Two_Component_Test
    Fuel_Comp ;
  FuelsDataAdjustable
    Data(Fuel_Comp=Fuel_Comp) ;
end Fuel;
```

The replaceable `Two_Component_Test` model defines the fuel. This model contains the injected mass fractions, the fuel names string, and an array of integers that specifies which components are used. This information is then passed to the `FuelsDataAdjustable` model. The `FuelsDataAdjustable` model extracts the material property data for the used species from the list of possible species. `FuelsDataAdjustable` is implemented as a model and not as a record because of an assert statement in the equation layer of the model. This forces `Fuel` to be a model because one of its used classes is a model and not a record. Knowing which fuel, and hence which species, will be used at translation time decreases the number of variables and run time.

Note that the connector definition has a string parameter `FuelNames`. The string `FuelNames` is a concatenation of abbreviations for the names of all the various fuel components that make up the current fuel model. An example of `FuelNames` for the indolene fuel model is: `"ispnt|ioctn|tolun|ndecn|cyhex|naph|ethylb"`. This is on the connector to assure

that all the parts of the model are using a consistent fuel model.

The control volumes used to represent the liquid fuel are placed inside a wrapper model. The wrapper model contains the fuel model and a thermal connector that is connected to a thermal model that predicts the temperature of the puddle. It also has two models that calculate the surface tension and the vapor pressure of the fuel mixture in the puddle from the puddle temperature and fuel properties. The geometry (area, height, perimeter) of the liquid puddle is calculated in the equation layer of the model. It also has a liquid fuel connector that is similar to the control volume connector:

```
connector LiquidMixture
  import Modelica.SIunits;
  parameter Integer n "# of species";
  parameter String FuelNames;
  SIunits.Mass m[n];
  flow SIunits.MassFlowRate mdot[n];
  SIunits.Pressure Pv[n];
  SIunits.Temperature T;
  flow SIunits.HeatFlowRate q;
  SIunits.DynamicViscosity mu;
  SIunits.SurfaceTension SurfTen;
  SIunits.Area A;
  SIunits.Height H;
  WallWetting.Types.Perimeter Pwet;
end LiquidMixture;
```

The liquid puddle model and liquid mixture connector allow all of the information pertinent to the puddle to be calculated in one place. This prevents, for example, both the evaporation and forward flow models from calculating the puddle geometry.

The FORTRAN version used liquid puddle models to represent the liquid fuel puddles – one on the intake valve, one on the cylinder, and two in the port (see Figure 1). The fuel in the port is split into two puddles – one downstream in the port near the valve and one upstream away from the valve and close to the injector. The downstream puddle is nominally hotter than the upstream port. The modular nature of Modelica permitted easy creation of two different models with different numbers of control volumes. One is identical to the FORTRAN wall wetting model with 4 puddles. Both 4-puddle models can be used to model engines with multiple intake valves, bifurcated and non-bifurcated ports, and charge motion control valves by the use of multipliers. For example, an engine with two valves and a bifurcated port with fuel injected evenly into both ports would have the amount of fuel injected divided by 2 and the amount of fuel vaporized multiplied by 2.

To model liquid fuel dynamics with EMVA it was necessary to use 7 control volumes because each cylinder has two intake valves and a single fuel injector. Only one cylinder puddle control volume was used, but all of the other puddles were doubled to represent the two intake valves. The use of 7 control volumes instead of 4 with multipliers was necessary because of certain EMVA modes that are non-symmetrical. One such mode occurs when the intake valves open on alternating cycles, but the single fuel injector sprays fuel into both ports on each cycle.

The FORTRAN version of the wall wetting model had a control volume to keep track of the fuel evaporated. Some versions of the Modelica wall wetting model have a separate control volume to keep track of the fuel that has been vaporized. Others simply convert the multicomponent evaporation mass flow rate into a single component mass flow rate that can be applied directly to the medium connectors that Ford uses for cycle simulation [2].

In addition to the fuel model, four different records are used to pass information to different sections of the model. They are passed down the hierarchy as replaceable records or models.

## Processes

The wall wetting model has several processes that add fuel to the liquid puddles, move the liquid fuel between the puddles, and remove the evaporated fuel. The dominant process is evaporation [3]. Each puddle is connected to the air-stream using an evaporation model. The evaporation model uses the Reynolds number of the flow over the puddle, the free stream gas state (temperature, pressure, composition), and puddle information from the puddle connector. It calculates a total mass convection rate from the puddle to the air stream. The evaporation mass flow rate is governed by:

$$\dot{m}_{evap} = Sh\rho_{mix} \frac{A_{puddle}}{d_{port}} D \ln\left(\frac{X_{fvp} - X_{fvi}}{1 - X_{fvp}}\right) \quad (1)$$

where Sh is the Sherwood Number (dimensionless concentration gradient which is dominated by the Reynolds Number),  $\rho_{mix}$  is the density of the air/fuel mixture in the gas phase directly above the puddle,  $A_{puddle}$  is the area of the puddle,  $d_{port}$  is the port diameter, D is the diffusion coefficient,  $X_{fvp}$  is the mass fraction of fuel in the vapor phase above the puddle, and  $X_{fvi}$  is the mass fraction of fuel vapor in the inlet stream. The total mass convection rate is divided among the various fuel components (species) in the puddle based on their mass fractions in the vapor phase.

Liquid fuel is added to the puddles via an injector model. The injector apportions the total fuel injected by means of data about the engine hardware (e.g. injector targeting info) and calibration parameters (e.g. how much fuel dribbles off of the injector as opposed to being sprayed). Most of the fuel during closed valve injection goes to the valve puddle and the downstream port puddle. During the rare event of open valve injection a large portion of the fuel goes directly to the cylinder puddle. The injector model also calculates an amount of fuel that is either vaporized or entrained in the air stream before it reaches the puddle. It does this by calculating a Roslin-Rammler distribution of the fuel droplet size in the injection spray. Then it assumes that all the drops under a certain diameter are entrained, and half of the drops between that size and a larger size are entrained. Both sizes are calibration parameters.

A forward flow model simulates the dragging effects of the air-flow in the port. The forward flow model moves liquid fuel from the upstream puddle to the downstream puddle, and liquid fuel from the downstream and valve puddles into the cylinder puddle. All of these flows are modeled by instances of the same flow model.

Using the mass flow rate of air in the port, the forward flow model makes several assumptions in order to calculate a mass flow rate. First, it is assumed that there is no slip at the surface between the puddle and the engine. Next, there is an equal shear force between the puddle and the air stream. Finally, there is a laminar flow distribution in the air and fuel film. The model then divides the total mass flow rate among the various fuel components in the puddle by their mass fractions in the puddle. The forward flow model also has an entrainment model similar to that in the injector model.

The process of backflow shattering is also modeled. This occurs at intake valve opening (IVO) when the pressure in the port at part throttle operating conditions is much less than that in the cylinder. At typical operating conditions, the cylinder pressure at IVO would be at atmospheric (100 kPa) and the pressure in the port would be about 50 kPa. This pressure difference produces a short duration but large magnitude, sometimes sonic, backflow event. This shatters the downstream and valve puddles. A percentage of the fuel that was shattered will be blown up into the port, a percentage will fall back into the puddle, and a percentage will be entrained in the air. The process is modeled as an event in Modelica. At IVO an event is triggered and a submodel calculates the redistribution of fuel. This information is then passed up to higher levels so that all of the control volume models are children. This model uses `reinit` statements to move the percentages among the various control volumes. This method is not entirely

satisfactory because the process is not completely represented in one submodel. We are currently evaluating the experimental impulse handling functionality in Dymola to rewrite the backflow shattering model.

### ***Thermal Warm-up Model***

One of the most important features in predicting transient A/F dynamics is good prediction of the temperature of the liquid fuel. The liquid fuel puddle is thin and is assumed to be in thermal equilibrium with the engine surface. The task is therefore to make a thermal model of the intake valve, seat, and cylinder walls. The Modelica version of the wall wetting model is essentially the same as the FORTRAN version [4]. The valve and valve seat are modeled by thermal capacitances connected by thermal resistances. This resistor-capacitor network is connected to the combustion gases, backflow gases, fresh charge gases, and coolant fluid via thermal convective resistances. Twenty-six thermal capacitances are used. Four are for the valve stem, three are for the valve seat, one is for a thermocouple, and 18 are for the valve head. The thermal capacitance and thermal resistance models are the `HeatCapacitance` and `HeatResistance` modes from the `HeatFlow1D` package found in the `ModelicaAdditions` library. The `Convection` model in the `HeatFlow1D` library was not suitable because the convection coefficient is a parameter. In our model the convection coefficient changes throughout the simulation so we made our own convection model with a variable convection coefficient. When a formal heat transfer library is available in the Modelica Standard Library, we will migrate our models to use the standard components.

The temperature of the valve puddle is calculated as a weighted average of the cells on the valve head. The downstream port puddle is connected to one of the seat cells. The upstream port puddle is connected to an average of the coolant and the seat.

### ***Interface with Cycle Simulation***

The original FORTRAN wall wetting model was not coupled or integrated into to a detailed engine cycle simulation model. Therefore simple but useful approximations for information such as in-cylinder pressure, burned gas temperatures, and in-cylinder and port air velocities were used as inputs.

The Modelica version of the wall wetting model was designed to permit integration with engine cycle simulations of varying complexity. The simplest cycle simulation would be to use the approximations that the original FORTRAN model uses. The next level of complexity would be to have a simple cycle simulation (e.g. using a single species ideal gas model, prescribed

burn model, and no in-cylinder heat transfer effects) to provide results for input to the wall wetting model, but not visa versa. A more complex cycle simulation could also be used (e.g. using a multiple species gas model with detailed property models, a predictive burn model, and in-cylinder heat transfer effects). Finally, the most complex form of integration would involve the two-way communication of results between the wall wetting model and the cycle simulation model. In other words, the cycle simulation would provide the wall wetting models with the necessary temperatures, pressures, air flow velocities, and heat transfer coefficients while the wall wetting model would provide the cycle simulation with the air/fuel ratio.

For our purposes we have built two versions of the wall wetting model. This first was for model verification. Here we used a simple cycle simulation that was coupled one way to the wall wetting model. Then for the camless application we chose a slightly more complex cycle simulation model (four gas species, thermodynamic relations by polynomial, prescribed burn, and no in-cylinder heat transfer effects) that was fully coupled to the wall-wetting model.

## **Actuator Model Development**

Both simplified and detailed models of the EMVA have been developed. The simplified model is incorporated into the wall wetting simulation of the camless engine, while the more detailed "stand-alone" model is used for actuator controls development.

The actuator, shown schematically in Figure 2, is comprised of an upper and lower electromagnet and a moving armature which pushes on the engine poppet valve. Compression springs of equal stiffness ( $k_s$ ) are placed above and below the armature, and are pre-loaded during assembly (by positioning the threaded top spring housing) to center the armature between the solenoid pole faces as shown in the left figure. During engine start-up, the valve is pulled from the center position to one of the pole faces corresponding to the open or closed position of the poppet valve. During normal engine operation, the armature and engine valve essentially operate as a reciprocating system. The motion during a transition from one pole face to the other is then primarily harmonic with the transition speed being determined by the effective armature/valve mass ( $m_{eff}$ ) and the effective stiffness ( $k_{eff}=2k_s$ ) of the upper and lower springs. The electromagnets are used to (1) hold the valve in either the open or closed positions position, and (2) to inject enough magnetic energy into the armature to overcome frictional losses during transitions.

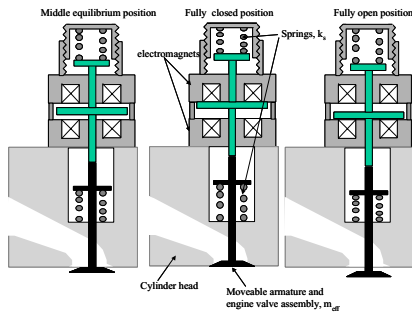


Figure 2: Schematic of the EMVA actuator in middle, fully open and fully closed positions.

### Simplified EMVA Model

A simplified sub-model is developed for use with the engine cycle simulations. The simplified model provides valve profiles to the valve port flow models which subsequently determine the gas flow to and from the engine cylinder. From a free-body diagram of the effective reciprocating mass  $m_{eff}$ , the equation of motion during a transition can be expressed in terms of the viscous friction damping coefficient  $c$ , the effective spring constant  $k_{eff}$ , the upper  $F_{mag,u}$  and lower magnet  $F_{mag,l}$  forces, and the gas pressure and flow forces  $F_{gas}$ :

$$m_{eff} \ddot{z} + c \dot{z} + k_{eff} z = F_{mag,u} - F_{mag,l} - F_{gas} \quad (2)$$

In Equation 2,  $z$  is the distance from the center position (the upper magnet face is at  $z = L/2$  and the lower magnet is at  $z = -L/2$ . Lift  $L$  is the total armature travel). The magnetic force drops off as with the square of the armature distance from the pole face; therefore, during most of the transition,  $F_{mag,u}$  and  $F_{mag,l}$  are small compared to the spring forces. Additionally, the damping coefficient is very small, and for light to moderate engine loads, the gas forces are relatively small. A reasonable first approximation to the valve lift  $x = z - L/2$  is harmonic motion at a frequency of  $\omega_n = (k_{eff}/m_{eff})^{1/2}$ . For example the position for movement from the closed position at time  $t_0$  is given by:

$$x = \frac{L}{2} (1 - \cos\{\omega_n(t - t_0)\}) \text{ for } t - t_0 \leq \pi/\omega_n \quad (3)$$

and

$$x = L \text{ for } t - t_0 > \pi/\omega_n \quad (4)$$

This simply generates a time based one-half period harmonic transition from closed to open position. A similar expression is used for the valve closing transition.

Figure 3 illustrates an instance of the simplified EMVA model within the context of the camless engine exhaust valvetrain model. The sub-model incorporates a rotational connector to sense engine position and a control connector that provides opening and closing timing signals from higher levels of the model. The output is the harmonic lift profile which is then connected to the exhaust port flow model.

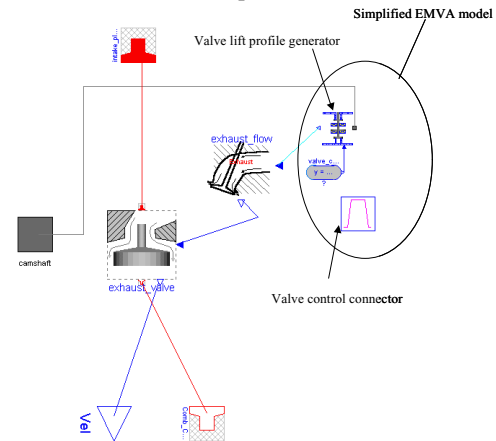


Figure 3: Exhaust valvetrain model showing the simplified EMVA model

### Detailed EMVA Model

Modelica standard libraries for linear masses and springs are used to model the mechanical characteristics of the system. Additionally a model of an E-core type electrical solenoid is developed and used in conjunction with the electrical libraries. This provides a plant model for evaluation of passive and active motion control schemes.

The model, shown in Figure 4, is used to evaluate the dynamics of the armature motion during catching near the end of a transition. It includes the mechanical system, a catching electromagnet, and simple voltage supply.

The mechanical system is modeled as a reciprocating mass that is connected to 4 spring-damper elements. These elements are piece-wise linear with a change in stiffness and damping coefficient defined by the positions where the armature meets the magnet pole face. Two of the spring-dampers represent the mechanical stiffness of the upper and lower actuator springs, while two other high-stiffness elements simulate the collision between the armature and the electromagnets. The lower stiffness spring-damper parameters are active during mid-travel ( $-L/2 < z < L/2$ ) and are tuned to match the free oscillation motion of the armature. The high stiffness spring-dampers (active for  $|z| \geq L/2$ ) are then tuned to match the experimental data to simulate the inelastic collision of the armature with either of the magnet pole faces.



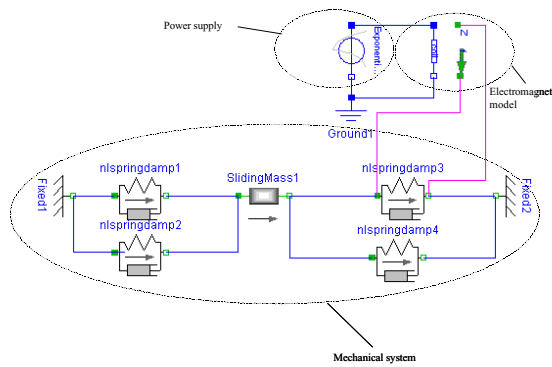


Figure 4: Actuator model

Also shown in Figure 4 is an e-core magnet sub-model. Electrical connectors are provided to connect the coils to a voltage source. In addition, a translational connector is provided to apply the magnetic force to the spring-mass-damper system.

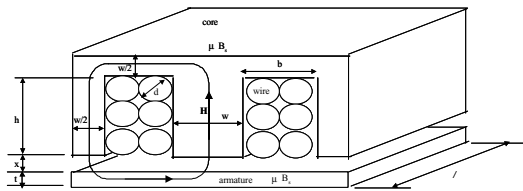


Figure 5: "E"-core magnet schematic

The magnet model development begins with a consideration of the e-core geometry and flux path, which is shown schematically in Figure 5. By applying Gauss' law for magnetostatics:

$$\oint \vec{B} \cdot d\vec{A} = 0 \quad (5)$$

where  $\vec{B}$  is the magnetic field and Ampere's law:

$$\oint \vec{H} \cdot d\vec{l} = I_{enclosed} = Ni \quad (6)$$

where  $H$  is the magnetic excitation,  $i$  is the current, and  $N$  the number of coil turns, the flux can be expressed in terms of the geometry, windings, material properties, air gap  $x$ , and current  $i$  for both the linear (where magnetic field  $\vec{B}=\mu\vec{H}$ ) and magnetic saturation regions of operation. In the linear region the flux is given by:

$$\lambda = \frac{ai}{k+x} \quad (7)$$

where  $a$  and  $k$  are constants determined by the core and armature dimensions and material properties.

Integrating  $\lambda$  with respect to current  $i$  gives the co-energy, which can be differentiated with respect to the air gap to give the magnetic force  $F_{mag}$ :

$$F_{mag} = \frac{ai^2}{2(k+x)^2} \quad (8)$$

The flux and magnetic force will vary according to Equation 7 and Equation 8 until either the core or armature begins to saturate at higher current levels. Here, an exponential form for the flux is defined which permits the characterization of the flux and magnetic force in terms of the B-H curve characteristic of the materials.

With the flux characterized, the equation which describes the voltage  $V_a$  applied across the coil the can be expressed using Kirchoff's, Faraday's and Ohm's laws:

$$V_a = \frac{d\lambda}{dt} + Ri \quad (9)$$

where  $R$  is the coil resistance which is parameterized in terms of the e-core dimensions and wire diameter  $d$ .

Equations for the magnetic force and the coil voltage essentially describe the magnet sub-models. The model interfaces with the electrical and mechanical subsystems through translational connectors and electrical pins.

## Results and Discussion

### Wall Wetting Simulations

The camless wall wetting model has been used to model 1200 RPM 300-second engine "cold-start" tests. The engine starts from near ambient conditions, and is then operated at 1200 RPM. The engine load (or torque) is periodically moved between a lower and higher level, with the excursions being made during a 1-second interval. The load changes are accomplished by changing the engine airflow induction rate. Both "throttled" and "unthrottled" operating modes are investigated, and simulation results are compared to experimental data. In the throttled mode, the camless engine is operated in a conventional way. The valve timings are fixed and load changes are executed by throttling the air flowing into the intake manifold. In the unthrottled mode, the intake manifold air is at atmospheric pressure. Load changes are accomplished by changing the intake valve closing timing (IVC) to change the length of the induction stroke.



Figure 6 shows the results for the throttled engine operation. Both experimental and predicted results are shown for injected air-fuel ratio (the ratio of inducted air mass per cycle to injected fuel mass per cycle) and for the air-fuel ratio in the engine exhaust (inferred from measuring exhaust species concentrations). Note that these are in general different under transient conditions due to the wall wetting fuel dynamics. The model prediction for injected air/fuel ratio is significantly higher than the experimental injected air fuel ratio during the high load operating condition. This difference may be attributed to modeling and experimental error. The difference could be due to over-prediction of the inducted air mass during high load conditions. The exhaust air fuel ratio for the experimental data and modeling simulation behave similarly during low load engine operation, but during high load operation conditions the experimental and modeled exhaust air fuel ratio diverge. This may be due to the differences in the injected air fuel ratios and experimental error.

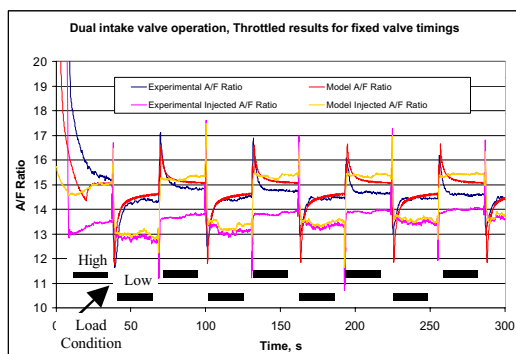


Figure 6: Throttled Operation.

Figure 7 shows the results for unthrottled engine operation. The injected air fuel ratio for the model closely matches the experimental data, demonstrating that the air charge estimation is improved compared to the throttled operating condition. However, the modeled exhaust air fuel ratio does not yield similar results. Although the experimental exhaust air fuel ratio tracks close to the desired stoichiometric conditions, the modeled exhaust air fuel ratio is calculated to be much richer. The model reasonably represents the air fuel excursions during load transitions, but most likely underestimates the quantity of fuel lost to the crankcase. If the model calibration of the lost fuel becomes more representative, the simulation is expected to more closely match the experimental results.

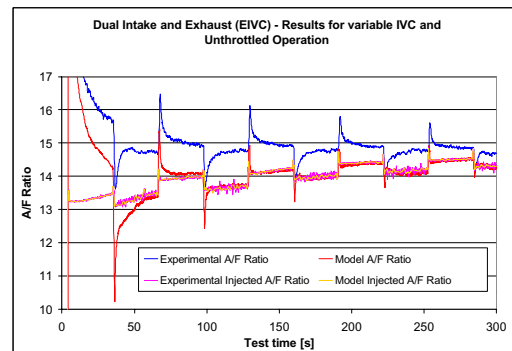


Figure 7: Unthrottled Operation.

These results show reasonable agreement for the general trends in air fuel-ratio behavior and demonstrate that Modelica is suitable for modeling transient air fuel dynamics; however, they also underscore the need for good model calibration and experimental air charge estimation. The FORTRAN version of the wall wetting model has a routine to calibrate the model by adjusting several parameters. The values of these calibrated parameters were used for the Modelica wall wetting model. However, the results show that the Modelica version of the model needs a different calibration process. Once a calibrated version of the model is available, it should be generally useful for both hardware and control strategy development.

### Actuator Simulations

The actuator model has been exercised to investigate various design and motion control scenarios. Here we present results that compare model predictions to experimental data for armature catching using a simple square-wave catching pulse.

The model flux and force relationships are tuned to e-core and armature properties for a 200V prototype actuator using data from [5]. Mass, spring and damping parameters are selected to provide reasonable agreement between the predicted and measured free oscillation data. Experimental data are obtained by using a bench-top experimental set-up described in [6]. An actuator is installed on a cylinder head, and instrumentation is provided to drive the coil and to measure the position, velocity, current, and voltage. Figure 8 illustrates the experiment. The actuator is held in either the open or closed position with a low holding current in the corresponding coil. This holding coil current is then quenched at the time of the release command. After a delay time  $t_d$ , a square wave catching pulse of amplitude  $V_{app}$  and pulse-width  $t_{pw}$  is applied to the opposite coil to catch the armature at the magnet pole face. The catching coil voltage is then decreased to provide the lower current required to hold the valve in position.

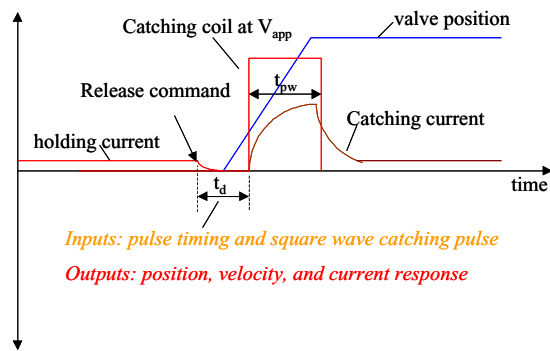


**Figure 8: Schematic of armature catching experiment.**

Figure 9 shows both predicted and measured position and velocity traces for a  $V_{app} = 117$  V,  $t_{pw} = 10$  ms catching pulse applied at  $t_d = 1.4$  ms from the armature release point. The release spring first accelerates the armature and valve assembly to peak velocity of about 3.7 m/s. As the armature approaches the coil seat, it decelerates due to the catching spring force, but the magnetic force increases to pull the armature in to the open position. The predicted and measured contact velocities are about 0.3 m/s and 0.5 m/s respectively, and occur at 3.2 ms from the release point. Note that under these conditions the armature bounces and contacts a second time at about 0.6 m/s at around 4.5 ms.

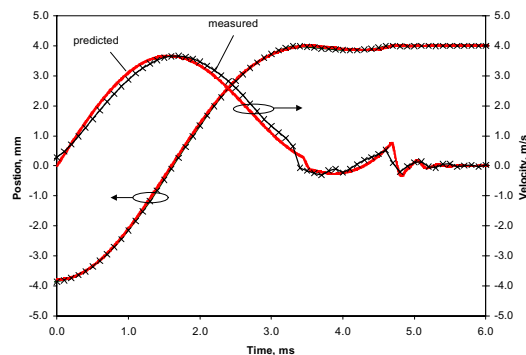


**Figure 9: Predicted and measured position and velocity for apply voltage  $V_{app} = 117$  V, delay time  $t_d = 1.4$  ms, and pulse-width  $t_{pw} = 10$  ms.**

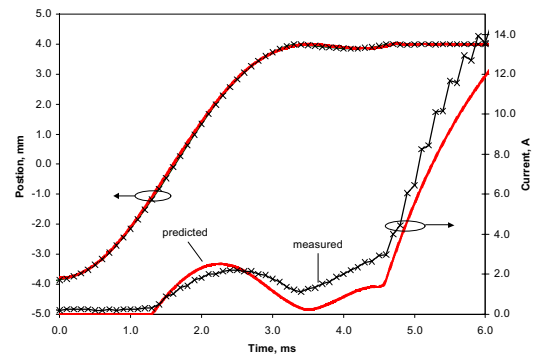


**Figure 10: Predicted and measured position and current for apply voltage  $V_{app} = 117$  V, delay time  $t_d = 1.4$  ms, and pulse-width  $t_{pw} = 10$  ms.**

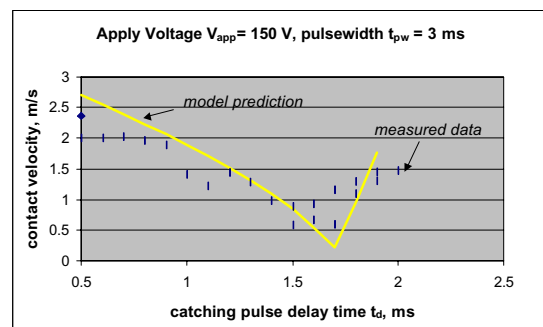


**Figure 11: Predicted and measured contact velocity versus catching pulse delay time  $t_d$  for apply voltage  $V_{app} = 150$  V and pulse-width  $t_{pw} = 3$  ms**

Figure 10 shows the predicted and measured current responses. The measured current first increases to about 2.0 amps, and then decreases as the armature lands due to the counter electromotive force (EMF) induced when the armature moves toward the magnet pole face. After bouncing, the armature moves away from the pole face and induces a reinforcing EMF. The current then increases, and this subsequently increases the magnetic force to pull the armature in with a higher contact velocity during the second impact. After the armature lands, the current then increases even more rapidly due to magnetic saturation effects. The model over-predicts current until very near the landing point. Here the model predicts a much sharper current decay than is shown by the measurement. The overall trends agree; however, model refinements are being developed to improve the current prediction.

An important issue for actuator design and control is the poppet valve and armature contact velocities. Valve seating velocities must be low enough so that valvetrain durability and noise level targets are met. Figure 11 shows the predicted contact velocities for the pulse timing sweep experiment shown in Figure 8. Here the applied voltage is  $V_{app} = 150$  V, the pulse width is  $t_{pw} = 3$  ms, and the pulse timing delay  $t_d$  is varied. As the pulse timing delay  $t_d$  is varied from 0.5

ms to 1.7 ms, the contact velocity decreases from about 2.7 m/s to a minimum of about 0.2 m/s. The minimum occurs when the injected energy from the magnetic force is about equal to the frictional losses from damping. For  $t_d > 1.7$  ms the contact velocity begins to increase (due to reinforcement of the coil current as the armature motion reverses near the landing point) until  $t_d = 2.0$  ms. Beyond this point, the magnetic force is not sufficient to catch the armature. Experimentally measured contact velocities are also shown in Figure 11. The predicted and measured trends agree reasonably well.

## Conclusion

The Modelica language proved to be useful for creating a model for transient fuel dynamics in port fuel injected engines. The model was easily integrated into a cycle simulation model, and was suitable for modeling the transient fuel dynamics in a camless engine, as the predicted trends agreed reasonably with measured data. Modelica was also useful for developing camless engine valve actuator models. An actuator model was developed by using an e-core solenoid sub-model and a mixture of elements from the standard translational and electrical libraries. The model predictions for valve motion agreed reasonably well with experimental data.

## References

1. Curtis, E., Russ, S., Aquino, C., Lavoie, G., Trigui, N., "The Effects of Injector Targeting and Fuel Volatility on Fuel Dynamics in a PFI Engine During Warm-Up: Part II – Modeling Results", SAE 982519
2. Newman, C., Batteh, J., Tiller, M., "Spark Ignited-Engine Cycle Simulation in Modelica", 2002 Modelica Conference Proceedings
3. Spalding, D.B., Combustion and Mass Transfer, Pergamon Press, 1979.
4. Curtis, E., Aquino, C., Plensdorf, W., Trumpy, D., Davis, G., Lavoie, G., "Modeling Intake Valve Warmup", ICE-Vol. 29-1, Proceedings of the 19<sup>th</sup> Annual Fall Technical Conference of the ASME Internal Combustion Engine Division, 1997.
5. Wang Y., Stefanopoulou A. G., Haghgoie M., Kolmanovsky I., Hammoud M., "Modeling of an Electromechanical Valve Actuator for a Camless Engine", AVEC 2000, 5th International Symposium on Advanced

Vehicle Control, No. 93, Ann Arbor, USA, 2000.

6. Wang Y., "Camless Engine Valvetrain: Enabling Technology and Control Techniques" Ph.D. Dissertation, University of California, Santa Barbara, 2001